THE CODING AND SMALL-NON-CODING HIPPOCAMPAL SYNAPTIC RNAome

Robert Epple[1], Dennis Krüger[1,2], Tea Berulava[1], Gerrit Brehm[3, 4], Rezaul Islam[1], Sarah Köster[3, 4] & Andre Fischer[1,4,5*]

[1]Department for Systems Medicine and Epigenetics, German Center for Neurodegenerative Diseases (DZNE), Von Siebold Str. 3a, 37075, Göttingen, Germany
[2]Bioinformatics Unit, German Center for Neurodegenerative Diseases (DZNE), Von Siebold Str. 3a, 37075, Göttingen, Germany
[3]Institute for X-Ray Physics, University of Göttingen, Göttingen, Germany
[4]Cluster of Excellence "Multiscale Bioimaging: from Molecular Machines to Networks of Excitable Cells" (MBExC), University of Göttingen, Germany
[5]Department of Psychiatry and Psychotherapy, University Medical Center Göttingen, Germany

*corresponding author: andre.fischer@dzne.de (ORCID: 0000-0001-8546-1161)

Abstract

Neurons are highly compartmentalized cells that depend on local protein synthesis. Thus, messenger RNAs (mRNAs) have been detected in neuronal dendrites and more recently also at the pre- and postsynaptic compartment. Other RNA species, such as microRNAs, have also been described at synapses where they are believed to control mRNA availability for local translation. Nevertheless, a combined dataset analyzing the synaptic coding and non-coding RNAome via next-generation sequencing approaches is missing. Here we isolate synaptosomes from the hippocampus of young wild type mice and provide the coding and non-coding synaptic RNAome. These data are complemented by a novel approach to analyze the synaptic RNAome from primary hippocampal neurons grown in microfluidic chambers. Our data show that synaptic microRNAs control almost the entire synaptic mRNAome and we identified several hub microRNAs. By combining the *in vivo* synaptosomal data with our novel microfluidic chamber system, we also provide evidence to support the hypothesis that part of the synaptic microRNAome may be supplied to neurons via astrocytes. Moreover, the microfluidic system is suitable to study the dynamics of the synaptic RNAome in response to stimulation. In conclusion, our data provide a valuable resource and hint to several important targets for future experiments.

Keywords: mRNA, microRNA, lncRNA, snoRNA, synapse, synaptosomes, gene-expression, RNA-sequencing

Introduction

Neurons are highly compartmentalized cells that form chemical synapses and the plasticity of such synapses is a key process underlying cognitive function. In turn, loss of synaptic integrity and plasticity is an early event in neuropsychiatric and neurodegenerative diseases. Synapses are usually far away from the soma, which raises the question how neurons ensure the supply of synaptic proteins. Theoretical considerations and a substantial amount of data show that mRNAs coding for key synaptic proteins are transported along dendrites to synaptic compartments, where they are locally translated into proteins (Doyle & Kiebler, 2011) (Kosik, 2016) (Holt *et al,* 2019) (Fonkeu *et al,* 2019) (Biever, 2020). Hence, several studies investigated the synaptic RNAome via different approaches. For example, early *in situ* hybridization experiments demonstrated the localization of specific mRNAs to synapses (Garner *et al,* 1988). In addition, microarray and RNA-seq techniques were used to study the synapto-dendritic (Cajigas *et al,* 2012) (Ainsley *et al,* 2014) (Farris *et al,* 2019), synapto-neurosomal (Most *et al,* 2015) and more recently also the synaptosomal RNA pool of the mouse brain (Chen *et al,* 2017) (Hafner, 2019). However, compared to mRNAs, there is comparatively less knowledge about the non-coding RNAome at synapses. The best known non-coding RNAs are microRNAs which are 19-22 nucleotide long RNA molecules regulating protein homeostasis via binding to a target mRNA thereby causing its degradation or inhibition of translation (Gurtan & Sharp, 2013). Several microRNAs have been implicated with synaptic plasticity and were identified at synapses where they have been linked to the regulation of mRNA stability and availability for translation (Smalheiser, 2014) (Weiss *et al,* 2015) (Rajman & Schratt, 2017) (Sambandan *et al,* 2017). The combined analysis of the synaptic microRNA/mRNAome is however lacking and knowledge about other non-coding RNA species is rare. Another issue is that the methods used so far to study synaptic RNAs from tissue samples do not allow to distinguish between RNAs produced by the corresponding neurons and RNAs that might be transferred to synapses from other cell types. This question is becoming increasingly important, since there is emerging evidence for inter-cellular RNA transport and data supporting the hypothesis that for example glia cells provide neurons with RNA (Sotelo *et al,* 2014) (Jose, 2015). In this study we isolated synaptosomes from the hippocampus of mice and performed from the same preparation total and smallRNA-sequencing. To complement these data and address the question about the origin of synaptic RNAs we developed a novel microfluid chamber that not only allowed us to grow primary hippocampal neurons that form synapses in a pre-defined compartment (Taylor *et al,* 2010), but enabled us to isolate the synaptic compartments from these chambers using a novel device we call SNIDER (**Sy**N**a**pse **I**solation **D**evic**E** by **R**efined Cutting) followed by RNA-sequencing. We also show that this novel microfluid chamber is suitable to assay the dynamics of the synaptic RNAome in response to stimulation. In conclusion, our experiments allowed us for the first time to build a high-quality synaptic microRNA/mRNA network and suggest key synaptic RNAs, including lncRNAs and snoRNAs, for future mechanistic studies in the context of the healthy and diseased brain.

Results

The hippocampal coding and non-coding synaptosomal RNAome

We isolated high-quality synaptosomes from the hippocampus of 3 months old mice, and processed the corresponding RNA for total and small RNA-sequencing **(Fig 1A)**. After quality control for high confidence transcripts we could detect 234 mRNA, 6 lncRNAs (excluding sequences that code for predicted genes), 65

microRNAs and 37 SnoRNAs **(Fig 1B, tables S1, 2, and 3)**. GO-term analysis revealed that the mRNAs reflect exclusively the pre-and post-synaptic compartment **(Fig 1C)** confirming the quality of our data. Functional pathway analysis showed that the mRNAs found in our synaptosomal preparations represent key pathways linked to synaptic function and plasticity **(Fig. 1D)**. We also observed a substantial amount of highly abundant microRNAs present in our synaptosomal preparations **(Table S2)** and wanted to understand the synaptic regulatory mRNA-microRNA network. To this end, we applied a novel bioinformatic approach and first generated the mRNA-network using the mRNAs detected at synapses, intersected this network with the synaptic microRNAome and asked if any of mRNAs within the network represent confirmed microRNA targets. Our data revealed that the 98% of the synaptic mRNAome is targeted by 95% of the synaptic microRNAs **(Fig 1E, F)**. These data suggest that the synaptic microRNAome plays an important role in local mRNA availability. We detected a number of hub microRNAs and especially micoRNA-27b-3p, microRNA-22-3p, the cluster consisting let-7b-5p, let-7c-5p and let-7i-5p as wells as microRNA-181a-5p, microRNA-9-5p and microRNA-124-5p appear as central regulators of the synaptic mRNA pool **(Fig 1F)**.

Comparison of the hippocampal synaptosomal coding and non-coding RNAome to primary hippocampal neurons

Compartmentalized microfluidic chambers have been developed to study the pre- and postsynaptic compartments of neurons. In these chambers, neurons grow their neurites into microgrooves and form synapses in a narrow compartment, the perfusion channel (Taylor *et al.,* 2010). We hypothesized that such microfluidic chambers would be a *bona fide* complementary approach to study the synaptic RNAome via RNA-sequencing. Moreover, since the synapses formed within the perfusion channel of such chambers are not in contact with any other neural cell type, this approach would also allow us to address the question to what extent synaptically localized RNAs originate from the corresponding cell or may have been shuttled from neighboring glia cells, a process that has been specifically proposed for synaptic microRNAs (Prada *et al,* 2018). However, a reliable approach to isolate synapses and corresponding RNA for subsequent sequencing from the perfusion channel of such microfluidic chambers did not exist. Therefore, we generated a modified microfluidic chamber that allowed us to cut the perfusion channel to harbor the corresponding synapses followed by the isolation of RNA. Thus, we grew mouse hippocampal neurons in these chambers **(Fig 2A)**. For reproducible cutting we employed a newly-devised instrument we call SNIDER (**Sy**napse **I**solation **D**evic**E** by **R**efined Cutting) **(Fig 2B, C)** and isolated RNA for total and smallRNA sequencing. When comparing the transcriptome obtained from the perfusion channel, with corresponding data generated from RNA isolated from primary hippocampal neurons grown in normal culture dishes, we observed the expected enrichment for a specific subset of RNAs, representing about 12% of the entire transcriptome **(Fig 2D)**. In more detail, the transcriptome of the perfusion chamber consisted of 1460 mRNAs, 199 lncRNAs, 54 microRNAs and 57 highly expressed snoRNAs of which 22 were also detected in synaptosomes. **(Fig 2E, Supplemental tables S4, 5, 6)**. GO-term analysis revealed that the identified mRNAs represent the synaptic compartment, which is in line with our data obtained from the adult mouse hippocampus **(Fig 2F)** and further supports the feasibility of our approach. Functional pathway analysis confirmed that the detected mRNAs code for key synaptic pathways and reflect the high energy demand of synapses (oxidative phosphorylation). This is also the reason why pathways such as Alzheimer's, Huntington's

and Parkinson's disease are identified **(Fig 2G)**, since key genes de-regulated in these diseases are linked to mitochondria function. The direct comparison of the hippocampal synaptic mRNAome from the adult mouse brain and the mRNAome from primary neurons revealed that almost all mRNAs detected from *in vivo* synaptosomes, are also found in primary neurons grown in microfluidic chambers **(Fig 2H),** confirming 219 mRNAs as a high-quality and reproducible synaptic mRNAome. The GO-terms and functional pathways linked to these 219 mRNAs are identical to the data shown in Fig 1C&D. The 1244 mRNAs that were specifically observed in microfluidic chambers represent also the synaptic compartments and pathways linked to oxidative phosphorylation, synaptic vesicle cycle and metabolic processes and may therefore reflect the difference of the synaptic RNAome in the adult brain and cultured primary neurons **(Fig 2I)**. In addition, "neuronal projection" is detected as a significant GO-term, most likely indicating the fact that unlike synaptosomal preparations, the perfusion channel still contains some neurites. This might also explain that much more lncRNA, namely 199 annotated lncRNAs, are detected in the microfluidic chambers. Pathway analysis suggest that these lncRNA are mainly linked to mRNAs that control processes associated with oxidative phosphorylation and synaptic plasticity while comparatively few microRNAs seem to be regulated by the synaptic lncRNAs (**Fig S2)**. Similar to the *in vivo* data, we found 54 highly expressed microRNAs **(Table S5).** To further study the mRNA/microRNA network, we used the same approach as described for the synaptosomal data. Our data reveals that the 88% of the synaptic mRNAome in microfluidic chambers is targeted by 45 (83%) synaptic microRNAs **(Fig 3A)**. Taken together, our data from hippocampal synaptosomes and the novel microfluidic chamber strongly suggest that the synaptic transcriptome is under tight control of a local microRNA network. Comparison of the *in vivo* synaptic microRNAome to the data obtained from the microfluidic chambers revealed 17 microRNAs that were commonly identified at synapses, while 37 microRNAs were specific to the chambers and 48 microRNAs were only found in the *in vivo* data from hippocampal synaptosomes **(Fig 3B)**. When we generated the synaptic microRNA/mRNA network for the commonly detected 17 synaptic microRNAs and 219 mRNAs (see Fig 2G), we observed that this core synaptic microRNAome controls 80 % (179 of 219) of the core mRNAome **(Fig 3C)**.

Evidence for astrocytic microRNA transport to synapses

The finding that 37 microRNAs are exclusively found in synapses from primary neurons is likely due to the difference between *in vivo* brain tissue and primary neuronal cultures and a similar trend has been observed at the level of the mRNAs **(see Fig 2G)**. More interesting is the observation that 73%, namely 48 out 65, of the microRNAs detected in hippocampal synaptosomes are not found in microfluidic chambers (see Fig 3B), which is in contrast to the mRNA data in which almost all of the synaptosomal mRNAs are also found in synapses of the primary neuronal cultures grown in microfluidic chambers (See Fig 2G). These data may indicate that *in vivo* some of the synaptic microRNAs are not exclusively produced by the corresponding neuron but might be rather shuttled to synapses via other neural cell types. In fact, movement of microRNAs between cells is an accepted mechanism of intra-cellular communication (Jose, 2015). Prime candidate cells to support synapses with microRNAs are astrocytes that form together with neurons tripartite synapses. A prominent mechanism that mediates RNA transport amongst neuronal cells is intracellular transport via exosomes (Smythies & Edelstein, 2013). Thus, we compared a previously published dataset in which microRNAs from astrocytic exosomes were analyzed via a TAQman microRNA-array (Jovičić *et al*, 2013). Indeed, 50% of the microRNAs exclusively

detected in hippocampal synaptosomes have also been described in exosomes released from astrocytes **(Fig 4A)**. When we asked if these 23 microRNAs have mRNA targets detected in synaptosomes we observed that 21 of these microRNAs target in total 197 out of the commonly detected 219 synaptic RNAs (**Fig. 4B)**, which is further confirmed by functional pathway analysis showing that the 21 microRNAs control synaptic genes linked to the glutaminergic synapse, LTP and cAMP signaling (**Fig. 4C)**. It is interesting to note that the synaptic mRNAs not targeted by any of the 21 microRNAs represented functional pathways linked to oxidative phosphorylation **(Fig. 4D)**.

Synaptic microRNAs are linked to neurodegenerative and neuropsychiatric diseases

So far, our data support the view that the synaptic microRNAome plays an important role in neuronal function. To further strengthen this notion, we decided to ask whether synaptic microRNAs might be particularly de-regulated in cognitive diseases. To this end we performed a literature search and curated a list of 71 microRNAs that were found to be de-regulated in post-mortem human brain tissue, blood samples or model systems for Alzheimer's disease, depression, bi-polar disease or schizophrenia. Comparison of this dataset with our findings from synaptosomes revealed 17 synaptic microRNAs that are de-regulated during cognitive diseases of which 4 are also found in the microfluidic chambers and 11 were also detected in astrocytic exosomes, representing an interesting pool of synaptic microRNAs for further studies **(Table 1)**.

Microfluidic chambers are suitable to assay the synaptic RNAome upon neuronal stimulation

Our findings suggest that we can study the synaptic RNAome in a reliable manner using our modified microfluid chambers in combination with SNIDER. This approach also provides a novel tool to study the neuronal-controlled synaptic RNAome in response to stimulation. To further evaluate this potential, we decided to expose primary hippocampal neurons grown in microfluidic chambers to KCl treatment followed by the isolation of the perfusion channel and RNA isolation for RNA-sequencing 2 h later **(Fig 5A)**. Our analysis revealed a substantial number of mRNAs that were increased in the synaptic compartment **(Fig 5B, Table S7)**. Since we can exclude that these mRNAs are shuttled from glia cells, they likely represent part of the transcriptional response and reflect mRNAs that were transported to synapses, which is feasible within the 2h time window after treatment. In line with this assumption the up-regulated RNAs exclusively represent the synaptic compartment **(Fig 5C)**. Functional pathway analysis revealed a strong enrichment of RNAs coding for the ribosome **(Fig 5D)**. In fact, 50% of all transcripts that correspond to the ribosomal subunits were increased at the synapse upon KCL treatment **(Fig 5E)**.

Discussion

The synaptic RNAome

The aim of our study was to provide a high-quality dataset of the synaptic coding and small non-coding RNAome with a specific focus on microRNAs. Thus, our data represents an important resource for future studies. To the best of our knowledge our study also provides the first dataset which analyzes in parallel the coding, non-coding and small non-coding RNAome in hippocampal synapses via next-generation sequencing. Moreover, we used two different approaches in that we isolate hippocampal synaptosomes from the

hippocampus of 3 months-old wild type mice and we developed a microfluidic chamber that in combination with a novel cutting device allowed us to isolate synaptic compartments for subsequent RNA-sequencing from primary hippocampal neurons. This chamber combines the advantages of the currently used microfluidic chambers that allow the specific manipulation of synapses (Taylor *et al.*, 2010), with the ability to isolate the perfusion channel that harbors synaptic connections. Therefore, this novel microfluidic chamber will allow the specific manipulation of the synaptic compartment in combination with next-generation sequencing approaches and should be viewed as a suitable screening tool to study the dynamics of the synaptic RNAome. Feasibility of this approach was for example demonstrated by our finding that KCL treatment leads to substantial changes of the synaptic RNAome and future approaches will now employ more physiological manipulations and study the synaptic RNAome in disease models. It is noteworthy, that most of the mRNAs up-regulated at the synapse upon stimulation represent key components of the ribosome, which is in agreement with the importance of local mRNA translation (Holt *et al.*, 2019).

In line with previous data we identified a substantial number of mRNAs that almost exclusively represent the synaptic compartment and key signaling pathways linked to synaptic integrity and plasticity. It is interesting to note that the mRNA coding for the amyloid-precursor protein (APP), a key factor in Alzheimer's disease (AD) pathogenesis, was also found at synapses **(see Table S1)**. To our knowledge, this observation has not been explicitly reported before but is in line with the physiological function of wild-type APP at synapses (Hefter *et al*, 2020). Generally, we detected more mRNAs within the dataset obtained from primary neurons when compared to the synaptosomal preparation. This observation likely reflects the difference between the *in vivo* preparation of hippocampal tissue and cultured primary neurons. Another important consideration is that synapses likely differ depending on the distance to the soma, an issue that cannot be addressed when isolating synaptosomes, while the RNAome detected in the microfluidic chambers represent synapses that are most distant to the corresponding somata. Similar important is the fact that the preparation from the perfusion channel of our microfluid chamber still contains some neurites. Thus, the corresponding RNAome also includes dendritic mRNAs. This view is supported by previous data in which the mRNA pool was analyzed from neuropil or synapto-dendritic compartments. For example, 2550 mRNAs were detected in hippocampal neuropil from mice (Cajigas *et al.*, 2012), and 1875 mRNAs where identified when ribosome-bound mRNA was analyzed in the same region (Ainsley *et al.*, 2014). We observed only 234 mRNAs in hippocampal synaptosomes but we suggest that these mRNAs represent a high-quality dataset. Thus, we only report mRNAs that passed rigorous quality control and exhibit a substantial amount of sequencing reads. The quality of these data is further confirmed by the fact that almost all of the synaptosomal mRNAs, namely 219, are also detected within the RNA-seq dataset we obtained from the microfluidic chambers. The most comparable mRNA dataset to our *in vivo* approach is a recent study that employed FACS to isolate synaptosomes from the mouse forebrain (Hafner, 2019) and also reported raw data on the generic synaptosomes. It is important to note that this study employed a different analysis pipeline and reported all transcripts that map with >25% of the read length when using the STAR-aligner tool, while we consider only transcripts that map with at least >66%. Nevertheless, we observed that the top 500 mRNAs reported by Hafner et al. almost completely overlapped with our dataset. Namely 209 of the 234 mRNAs that we reported for hippocampal synaptosomes are also found in the Hafner et al. dataset from mouse forebrain synaptosomes **(table S8)**, further supporting the quality of our dataset and

strengthening the view that synaptic mRNAs play a critical role in neuronal function. We also report the detection of lncRNAs in datasets obtained from synaptosomes and microfluidic chambers but for now restricted the presented data to the currently annotated lncRNAs. We also detected lncRNAs that are currently still referred to as "predicted" and await further confirmation. Therefore, we encourage researchers to further explore our raw data as annotation of the genome improves. The presence of lncRNA in synaptosomes is in line with previous data (Chen *et al.*, 2017) but it is interesting to note that more lncRNAs were found in the microfluidic chambers when compared to the *in vivo* synaptosomes. A similar trend has been observed for mRNAs and might be due to the fact that the RNA preparation from the microfluid chambers also contain some dendritic RNA. Our data suggest that the detected lncRNAs regulate processes associated with oxidative phosphorylation and synaptic plasticity and may also affected the function of selected microRNAs. Although these observations need to be further studied, it is interesting to note that metastasis-associated lung adenocarcinoma transcript 1 (Malat1) appeared as one hub lncRNA at synapses. This is in line with a previous study showing that knocking down MALAT1 in hippocampal neurons decreases the number of synapses, although it has to be mentioned that the authors linked this finding to the role of MALAT1 on gene-expression control (Bernard *et al,* 2010). The presence of snoRNAs at synapses is also highly interesting and in line with a previous study that reported snoRNAs in synaptosomes (Smalheiser *et al,* 2014). Moreover, there was a substantial overlap of the snoRNAs detected in synaptosomes and in primary neurons (60% of the synaptosomal snoRNAs were also detected in microfluidic chambers). Most of the commonly detected snoRNAs were of the C/D box (49%) or H/ACA-box type (17%) that regulate RNA-methylation and pseudouridylation of mainly ribosomal RNAs (Bratkovič *et al,* 2020), which is in line with the presence of ribosomes at synapses (Holt *et al.*, 2019). However, we also identified snoRNAs that cannot be classified in either category (35%) that warrant further investigation. Some of the synaptic snoRNAs have been associated to additional processes and for example SNORD50, SNORD83B or SNOR27 have been linked to mRNA 3' processing and post-transcriptionally gene-silencing (Bratkovič *et al.*, 2020), while SNORD115 affects mRNA abundance and is genetically linked to the Prader-Willi-syndrome, a rare genetic disease leading to intellectual disability (Cavaillé, 2017).

A synaptic mRNA/microRNA network.

We detected a substantial number of microRNAs in hippocampal synaptosomes and in the microfluidic chambers. The presence of mature microRNAs at synapses is in line with previous reports that employed RT-PCR to study neurites of primary hippocampal neurons (Kye *et al,* 2007), micro-array-technology to analyze microRNAs in the synapto-neurosomes isolated from the forebrain of mice (Lugli *et al,* 2008) or more recently also smallRNA-sequencing and NanoString analysis of hippocampal neuropil or synaptosomes (Smalheiser *et al.*, 2014) (Sambandan *et al.*, 2017). Comparison of the dataset generated by Sambandan and colleagues revealed that out of the 65 microRNAs we detect, 57 were also reported in this previous study. These data further strengthen the view that microRNAs play an important role at synapses and suggest that our dataset represents a high quality synaptic microRNAome as a resource for future studies. To the best of our knowledge, our study is the first that provides a synaptic coding and small non-coding RNAome from the same preparation thereby allowing us the address the role of the synaptic microRNAome at the systems level. We used the data

to develop a novel tool which is first fed with the mRNA data to parse multiple databases containing experimentally validated interactions and thereby building a high confidence mRNA network of the synapse (See methods for more details). We intersected this mRNA network with the confirmed targets of all microRNAs, which are detected within the same sample to build the synaptic microRNA/mRNA network. Overall, our data suggest that up to 98% of the synaptic mRNAome is controlled by synaptic microRNAs, suggesting that essentially all synaptic localized mRNAs are potentially regulated via the synaptic microRNAs. Considering that mRNA transport to synapses is an energy-demanding and highly controlled process (Doyle & Kiebler, 2011) it is likely that synaptic microRNAs do not degrade their mRNA targets but rather control their availability for local translation, a question that should be studied in future experiments at the systems level. Another important observation is that many of the synaptic microRNAs are de-regulated in cognitive diseases (see table 1) that often start with synaptic dysfunction. In addition, there is increasing interest in circulating microRNAs as biomarkers for cognitive diseases (Rao *et al,* 2013) (Rupaimoole & Slack, 2017). The fact that microRNAs have also been reported in synaptic vesicles (Xu *et al,* 2013) and in exosomes derived from neuronal cultures (Jain *et al,* 2019) suggest a potential path how pathological microRNA changes observed in the brain may also manifest in circulation. Hence, the various CNS clearance systems (Plog & Nedergaard, 2018) might transport such vesicles to the circulation, a hypothesis that should be further studied. In the same context, there is substantial data to suggest that microRNAs regulate biological processes across cell-types and even organs (Valadi H, 2007) (Jose, 2015). Intriguingly, in the perfusion channel of microfluidic chambers, which are free of any somata and only contain distal synapses and some neurites, substantially less microRNAs are existent than in the synaptosomes. These microRNAs significantly overlapped with the ones detected in exosomes released by astrocytes (Jovičić *et al.,* 2013). It is therefore tempting to speculate that within the tripartite synapse astrocytes support synapses with additional microRNAs that help to control the synaptic mRNA pool. Support for this view stems also from the observation that the 3 most significant functional pathways controlled by the synaptosomal microRNAome are "Glutamatergic synapse", "cAMP signaling" and "long-term potentiation", which are identical to the top 3 pathways controlled by the microRNAs that are potentially shuttled to synapses via astrocytes. These data underscore the importance of the corresponding mRNA pool and may suggest that microRNAs supplied to synapses by other cell types might suppress translation of the most relevant local mRNAs rather than degrading a few selected RNAs. Our data allowed us to identify a number of synaptic hub microRNAs (e.g. see Fig 1E and F) and the functional analysis of these microRNAs would be an important task for future studies. Of particular importance would be microRNAs that are de-regulated in cognitive diseases. Support for this view stems from recent data on microRNA-181a-5p, a hub in our synaptic network, that is de-regulated in neurodegenerative and neuropsychiatric diseases (Stepniak *et al,* 2015) (Ansari, 2019) and was found to be processed at synapses upon neuronal activity (Sambandan *et al.,* 2017). The finding that most microRNAs of the let-7 family are highly abundant at synapses and control a large set of mRNAs is also interesting is interesting, since these microRNAs have been observed in several CNS-related pathologies (Derkow *et al,* 2018) while comparatively little is known on their role on the adult brain. Another hub microRNAs is miR-125b-5p that is de-regulated in Alzheimer's disease and causes memory impairment in mice when elevated in the hippocampus of mice (Banzhaf-Strathmann *et al,* 2014), yet its role at the synapse remains elusive. Similarly interesting is miR-128-3p, that is de-regulated in various

316 neuropsychiatric and neurodegenerative diseases and recent data suggest that inhibition of microRNA-128-3p
317 can ameliorate AD pathology (Liu *et al,* 2019).
318 In conclusion, our study provides the synaptic RNAome and is thus a valuable resource for future studies. Our
319 data furthermore support the importance of synaptic mRNAs and microRNAs and we introduce a new
320 microfluidic chamber that will allow researchers to combine the power of a specific analysis and manipulation
321 of the synaptic compartment (Taylor *et al.*, 2010) with RNA-sequencing approaches.
322
323 **Materials & Methods**
324 *Animals*
325 Three months old male C57B/6J mice were purchased from Janvier Labs. All animals were housed in standard
326 cages on 12h/12h light/dark cycle with food and water ad libitum. All experiments were performed according
327 to the protocols approved by local ethics committee
328
329 *Isolation of hippocampal synaptosomes for RNA-sequencing.*
330 To obtain sufficient RNA for sequencing of hippocampal synaptosomes we isolated the hippocampi from sixty
331 3-month-old wild type mice. Twenty bi-lateral hippocampi were pooled as 1 sample to obtain 3 independent
332 samples that were further processed to isolate high-quality synaptosomes using a previously described
333 protocol (Boyken *et al*, 2013). In brief, hippocampi were homogenized by 9 strokes at 900 rpm in sucrose buffer
334 and centrifuged at 4° for 2min at 5000rpm (SS34). Supernatants were further centrifuged at 4° for 12min at
335 11000rpm. Pellets were loaded onto a Ficoll gradient and centrifuged at 4° for 35min at 22500rpm (SW41). The
336 interface between 13% and 9% Ficoll was washed by further centrifugation and then pelleted by 8700rpm for
337 12min in a SS34 rotor. Resuspended synaptosomes were then centrifuged on a sucrose gradient for 3h at
338 28000rpm (SW28). Finally, synaptosomes were fractioned via the Gilson Minipuls and 21 fractions were
339 collected and analyzed by dot blotting. For this, from each fraction, 2µl of sample were pipetted on
340 nitrocellulose membrane, and dried for 5min. Blocking of unspecific signal was done by 5% low fat milk in TBST
341 for 10 min. Antibodies against Synaptophysin and PSD95 were applied for 15min, then the membrane was
342 washed three times for 3min each, in TBST with 5% milk. Secondary antibody was applied for 15min.
343 Afterwards membrane was washed again three times with TBST without milk before being imaged. Only 5
344 fractions from each preparation showed a signal for synaptophysin and PSD95 ensuring the presence of high-
345 quality synaptosomes and were therefore processed for total and small RNA-sequencing.
346
347 *Production of microfluidic chambers*
348 To isolate synapses and corresponding RNA for subsequent sequencing from the perfusion channel of currently
349 employed microfluidic chambers (Taylor *et al.*, 2010) was not possible. Therefore, we generated a microfluidic
350 chamber that allowed us to cut the perfusion channel by using polydemethylsiloxan (PDMS) for the chamber
351 and the corresponding substrate **(Fig S1)**. Pilot studies showed that unlike the commonly used microfluidic
352 chambers (Taylor *et al.*, 2010), the usage of PDMS as a substrate to bind the chambers on allowed us to cut the
353 perfusion channel. In more detail, the microfluidic chambers were designed using AutoCAD 2017. The overall
354 layout was similar to the version reported by Taylor and colleagues (Taylor *et al.*), yet for more yield of synaptic

RNAs the length of the chamber was increased, with more microgrooves and a wider synaptic compartment to allow easier alignment during cutting. Layouts were translated into photolithography masks by Selba. Production of silicon wafers was done with two layers. The first layer was made by applying 2 ml Photoresist SU-8-2025 on 50.8mm diameter silicon wafers and running the spin coater with the following settings: 1.) 15 sec, 500 rpm, 100 ramp 2.) 100sec, 4000 rpm, 50 ramp. To prebake, wafers were put on a 65° heating plate for 1 min, then for 15min on a 95° heating plate. For depositing the first layer, the mask with the microgrooves pattern was inserted into the MJB4 mask aligner; exposure was set to 9 sec under light vacuum conditions. Afterwards wafers were postbaked at 65° for 1 min and 5 min at 95°C.

Subsequently 3 ml of the second photoresist SU-8-2050 were added on top and spread thin with the following spincoater protocol: 1.) 15 sec, 100 ramp, 500 rpm 2) 60 sec, 900 rpm, 50ramp. This time prebaking was done with 1min at 65° and minimum of 30min at 95°. The second layer was aligned to the microgrooves using the microscope of the mask aligner. UV light exposure lasted 19 sec, in the soft contact setting. After postbaking as described for the first layer, wafers were developed for 10min or more in mrDev600 with the aid of ultrasonication. PDMS (SYLGARD™ 184 Silicone Elastomer Kit) was used to manufacture the chambers as well as the bottom substrates. Sylgard components were mixed 10:1, mixed with a 1ml pipette tip, poured over the wafers that were placed in 6cm diameter Petri dishes and very thinly (1-2mm high) onto 10cm dishes. Degassing was done for minimum 15 minutes in a desiccator under vacuum. Afterwards wafers and bottom parts were transferred to a 70° oven and cured for 2h. Chambers and bottom parts were cut out by a scalpel, holes in the chambers were punched by biopsy punchers of 6mm and 8mm diameter and bottom parts were cut into smaller pieces to hold one chamber each. To clean off dust, the pieces off of dust they were placed in an ultrasonic bath for 10 min and then dried on a heatplate at 70°. PDMS can be bound to PDMS covalently under oxygen plasma conditions; a tesla-coil type device, the Corona plasma treater from Blackhole lab, was used to this end. The plasma treater was hovered slowly 2cm above the chambers (bottom side up), going back and forth to cover the whole area by discharges for 30sec, then the same was done to the bottom part. Thereupon both parts were brought together and pressed very slightly to ensure complete contact. Covalent bond forming was enhanced by placing the so assembled chamber in the oven at 70° for 10min. Subsequently chambers were filled with PBS or borate buffer to maintain hydrophilic properties. For chambers that were supposed to be imaged, chambers were not treated with plasma; rather chambers were assembled to the PDMS or glass substrate under the biosafety cabinet by simply pressing both pieces together. Once assembled, chambers were brought to a biosafety cabinet and washed with 70% ethanol, then twice with water. Coating on PDMS worked best when done with 0.5 mg PDL in borate buffer overnight. Visual inspection under the microscope should make sure that no bubbles are present in the chambers. Great care needs to be taken when washing to not remove the coating. Liquid should be never removed with a suction pump sucking liquid directly from the channels, instead liquid should be removed by pointing the pipette at the wall of open reservoirs. Washing was done twice with PBS, 80µl per top reservoir, allowing for the liquid to flow into the down reservoir. Perfusion reservoirs were washed by applying 50µl in each well, one at a time and waiting for 5min in between. Once all PBS was removed from the open reservoirs 80µl of medium was added per top reservoir, allowing for the liquid to flow into the down reservoir. This process was repeated once, before chambers were left over night in the incubator before seeding, to ensure proper hydrophilicity. For easier handling always two

chambers were put together in a 10cm dish, with two lids of 15ml falcon tubes filled with water next to them, to reduce the evaporation from the chambers themselves.

Primary hippocampal neuronal cultures

Pregnant CD1 mice were sacrificed under anesthesia by cervical dislocation at E16 or E17. Brains from embryos were extracted and their hippocampi collected. Processing was done using the Papain kit from Worthington, and cells were counted and diluted to a density of 5 Million per ml. Seeding was done with the following pipetting scheme in order to make sure, most cells reach the microgrooves but do not enter them. 10µl of cell suspension containing 70.000 cells were injected in the channels from the top wells. We started with the axonal side. A second pipetting step with 5µl added to the channels from the bottom wells, after inspection of cells under the microscope. After 10 minutes, a similar seeding was performed for the dendritic side. One hour later each well was filled up to 100µl. The next day another 100µl were pipetted into each well. Visual inspection under a microscope was necessary to do several rounds of seeding with decreasing volume to made sure the desired spread of cells was achieved. After two hours reservoirs of the chambers were filled up with medium to 100µl each, by pipetting an additional 70µl simultaneously in both reservoirs per side, while not adding more medium to the perfusion. We used Neurobasal Plus with GlutaMax, Penicilin/Strep and B27 Plus supplement for better viability. Parallel to chambers, normal 12-well dishes, coated with PDL in borate overnight and washed three times with water, were cultured at 260.000 cells per well; those served as standby cultures. Since medium evaporation can happen quickly in the chambers, every 2-3 days medium from these standby cultures was filtered by a 0.22µm syringe filter and then added to the chambers. For the KCl stimulation, around 50µl of medium was collected from each reservoir of the chambers, mixed with KCl as to result in a final concentration of 50mM when given back to the chamber and then incubated for 2h before RNA isolation.

Harvesting of synaptic RNAs from microfluidic chambers: SNIDER

In order to parallel cut the PDMS substrate, we designed a machine consisting of a blade-holding arm on a ball-bearing rail, allowing frictionless mobility in one dimension. A screw-driven spring drives the razorblades height position and allows for controlling the penetration depth of the blades into the PDMS. The non-cutting corners of the razorblade were removed with a plunger to only have one accessing point of the blades into the PDMS. Small metal plates were put in between the blades and served as spacers, increasing the inter-blade distance to 900 µm. On the day of harvest cells in the chambers were washed once with PDMS and flipped upside down. Great care was taken to maintain a RNAse free environment by prior cleaning of all tools and instruments with RNAsezap and 70% EtOH afterwards. To have an endpoint for the long parallel cut we introduced with a scalpel two horizontal cuts between the outer perfusion wells and the upper left respectively upper right well that met at the perfusion stream. Then chambers were aligned by their perfusion stream on a marked line of the device. By close visual inspection the blades were lowered just before entering the PDMS material and blades were brought in parallel to the synaptic compartment. Blades were then lowered 2mm deep into the substrate just before the perfusion outlet and then the metal lever was pulled backwards, moving the blades towards the perfusion wells until the parallel cut met the V-shaped cut induced by scalpel earlier. With a pair of

tweezers, the synaptic compartment was taken out and put into cell lysis buffer solution of GenElute Sigma kit, whereupon we followed the manufactures protocol under 1C to isolate total RNA, including small RNAs.

RNA sequencing

The synaptosomal RNA samples were split into halves; one was further processed to obtain total RNA libraries using the Illumina Truseq total RNA kit, the other half was used for small RNA sequencing using the NEBNext Small RNA Library Prep Kit as described before (Benito *et al,* 2015). For total RNA sequencing of RNA from microfluid chambers, we always pooled two samples and libraries were created with Takara´s SMARTer Stranded Total RNA-Seq Kit v2 - Pico Input Mammalian. small RNA libraries were generated using Takara´s SMARTer smRNA-Seq Kit for Illumina. To verify the library and sequencing procedure we added spike-in RNAs from the QIAseq miRNA Library QC kit prior to library creation.

Bioinformatic analysis

Sequencing data was processed using a customized in-house software pipeline. Illumina's conversion software bcl2fastq (v2.20.2) was used for adapter trimming and converting the base calls in the per-cycle BCL files to the per-read FASTQ format from raw images. Quality control of raw sequencing data was performed by using FastQC (v0.11.5). Trimming of 3' adapters for smallRNASeq data was done using cutadapt (v1.11.0) (https://doi.org/10.14806/ej.17.1.200). The mouse genome version mm10 was used for alignment and annotation of coding and non-coding genes. Small RNAs were annotated using miRBase (Griffiths-Jones, 2006) for miRNAs and snOPY (Yoshihama *et al,* 2013) for snoRNAs. For totalRNASeq reads were aligned using the STAR aligner (v2.5.2b) (Dobin *et al,* 2013)and read counts were generated using featureCounts (v1.5.1) (Liao *et al,* 2014). For smallRNASeq reads were aligned using the mapper.pl script from mirdeep2 (v2.0.1.2) (Friedländer *et al,* 2012) which uses bowtie (v1.1.2) (Langmead & Salzberg, 2012) and read counts were generated with the quantifier.pl script from mirdeep2. All read counts were normalized according to library size to transcript per million (TPM). We used a TPM cutoff of 1000 reads for smallRNAs to make sure that these smallRNAs were considerably detected up to an average raw count of 10 reads. To account for differences in sequencing depth between synaptosomal mRNAs (average of 6mio unique reads per lane) and mRNAs from microfluidic chambers (average of 20mio unique reads per lane) we applied a cutoff of 50 and 100 normalized reads, respectively. Differential expression analysis was performed with the DESeq2 (v1.26.0) R (v3.6.3) package (Love *et al,* 2014), here unwanted variance was removed using RUVSeq (v1.20.0) (Risso *et al,* 2014). Networks were build using Cytoscape (v3.7.2) (Shannon *et al,* 2003) based on automatically created lists of pairwise interactors. We used in-house Python scripts to detect interactions between expressed non-coding RNAs (miRNAs, lncRNAs, or snoRNAs) and coding genes; interaction information was collected from six different databases: NPInter (Teng *et al,* 2020), RegNetwork (Liu *et al,* 2015), Rise (El Fatimy *et al,* 2018), STRING (Szklarczyk *et al,* 2019), TarBase (Karagkouni *et al,* 2018), and TransmiR (Tong *et al,* 2019). All interactions classified as weak (if available) were excluded. The lists of pairwise interactors were loaded into Cytoscape and all nodes connected by only one edge were removed to build the final network, respectively.

Imaging

Cells were fixed in 4% PFA in PBS plus 1µM MgCl2, 0.1 µM CaCl2 and 120mM Sucrose. Our imaging setup consists of a Leica DMi8 microscope that is equipped with a STEDYcon. Phase contrast images were obtained using the Leica in its normal mode, with the Leica DMi8 software. All other fluorescent images were taken with the STEDYcon in either confocal or STED mode. Antibodies: PSD95 (Merck - MABN 68) and Synaptophysin 1 (Synaptic Systems 101 004), both diluted to 1:400. Secondary antibodies were StarRED (Abberior, STRED-1001-500UG) and Alexa Fluor 633 Anti-Guinea Pig (Invitrogen, A21105) both diluted to 1:400. DAPI was applied for 1min for counterstaining.

Availability of data

All sequencing data are available via GEO database. GSE159248:
https://www.ncbi.nlm.nih.gov/geo/query/acc.cgi?acc=GSE159248

Code availability

Not applicable

Compliance with Ethical Standards

The authors declare no conflict of interest. This work includes experiments with mice. All described experiments approved by the local animal care committee.

Consent to participate

Not applicable since this study does not involve research on human subjects.

Consent for publication

Not applicable since this study does not involve research on human subjects.

Funding

This work was supported by the following third-party funds to AF: the ERC consolidator grant DEPICODE (648898), funds from the SFB1286 (B06), the DFG under Germany's Excellence Strategy - EXC 2067/1 390729940 the and funds from the German Center for Neurodegenerative Diseases (DZNE).

Author contribution

All authors contributed to the study conception and design. RE conducted cell culture and RNA-sequencing experiments, build microfluidic chambers and analyzed data. DMK performed bioinformatic analysis, TB isolated synaptosomes, GB and SK helped with the generation of microfluidic chambers, RI performed total RNA-sequencing from hippocampal neuronal cultures in normal culture dishes and curated the disease-related list of microRNAs, AF supervised the project and wrote the manuscript.

Acknowledgments

RE is a members of the international Max Planck Research School (IMPRS) for Neuroscience, Göttingen. We thank Mike Zippert and Reinhard Hildebrandt for the construction of SNIDER. This work was supported by the

following third-party funds to AF: the ERC consolidator grant DEPICODE (648898), funds from the German research foundation (DFG) SFB1286 (B06) and funds from the German Center for Neurodegenerative Diseases (DZNE). SK is supported by the DFG via SFB1286 (B02). AF and SK are supported by funds from the DFG under Germany's Excellence Strategy - EXC 2067/1 390729940.

Figure legends

Figure 1: The coding and small-non-coding RNAome of hippocampal synaptosomes. A. Experimental scheme. **B.** Bar graph showing the detected RNA species. **C.** GO-analysis showing that the identified mRNAs represent the synaptic compartment. **D.** KEGG-pathway analysis showing that the synaptic mRNAome consists of transcripts that are essential for the function of hippocampal synapses. **E.** microRNA-mRNA interaction network of the synaptic RNAome. Red circles represent the identified mRNAs that form a highly connected network, while blue circles indicate the detected microRNAs. Only the names of the top hub microRNAs are shown. **F.** Heat map showing the synaptic microRNAome ranked by their confirmed mRNA targets that were found at synapses.

Figure 2: Analyzing the synaptic RNAome in microfluidic chambers via RNA-sequencing. A. Microfluid chambers build from PDMS. Left panel shows the scheme of the microfluidic chamber indicating the perfusion channel in which most of synapses form. The principle is based on chambers first reported by Taylor and colleagues (Taylor *et al.,* 2010) but has been substantially modified (See Fig S1 for more details). The middle panel shows the bright-field image of neurons growing in these chambers and the right panel shows immunostaining for PSD-95 and Synaptophysin within the perfusion channel (upper image) and the part of the chambers that contains the cell bodies (lower image). **B** Scheme and image showing our newly devised tool for cutting the perfusion channel from the microfluidic chambers, named SNIDER. **C.** Schematic illustration of the cutting of the microfluidic chambers. **D.** Venn diagram showing the comparison of the total RNA-seq data obtained from primary hippocampal cultures grown in normal dishes (primary neuronal culture) and corresponding data obtained from the perfusion channel isolated from microfluidic chambers in which primary hippocampal neurons were grown. **E.** Bar chart showing the detected RNA species. **F.** GO-analysis showing that the identified mRNAs represent the synaptic compartment. **G.** KEGG-pathway analysis showing that the synaptic mRNAome consists of transcripts that are essential for the function of hippocampal synapses. **H.** Venn diagram showing the overlap of mRNAs detected in hippocampal synaptosomes and in microfluidic chambers. **I.** Upper panel: GO-analysis showing that the 1244 mRNAs specifically detected in microfluidic chambers represent the synaptic compartment and "cell projection". Lower panel**:** KEGG-pathway analysis of the same dataset.

Figure 3: A core synaptic microRNAome. A. microRNA-mRNA interaction network of the synaptic RNAome detected in microfluidic chambers. Red circles represent the identified mRNAs that form a highly connected network, while blue circles indicate the detected microRNAs that control this network. Only the names of the top hub microRNAs are shown. **B.** Venn diagram comparing microRNAs detected in microfluidic chambers (Chambers) and synaptosomes. **C.** microRNA-mRNA interaction network of the 219 synaptic mRNAs commonly

detected in synaptosomes and microfluidic chambers and the 17 commonly detected microRNAs. Only the names of the top hub microRNAs are shown.

Figure 4: Comparing microRNAs from astrocytic exosomes to the synaptic RNAome. A. Venn diagram comparing the 48 microRNAs exclusively detected in synaptosomes to the list of microRNAs found in astrocytic exosomes. **B.** microRNA-mRNA interaction network showing that 203 of the commonly detected 219 mRNAs and 21 of the 23 microRNAs found in synaptosomes and astrocytic exosomes form an interaction network. Only the names of the top hub microRNAs are shown**. C.** KEGG-pathway analysis of the 203 mRNAs within the network. **D.** KEGG pathway analysis of the 16 common synaptic mRNAs that are not targeted by the overlapping microRNAs shown in (A).

Figure 5: The synaptic mRNAome upon stimulation. A. Experimental scheme. **B.** Volcano plot showing a substantial up-regulation of synaptic RNAs upon KCL treatment. **C.** GO-analysis showing that the identified mRNAs represent the synaptic compartment. **D.** KEGG-pathway analysis showing that the changes of the synaptic mRNAome upon KCL treatment represent transcripts mainly linked to ribosomal function. **E.** Upper panel shows images of the KEGG pathway for "ribosome". Colored subunits represent transcripts significantly increased. Lower panel: bar chart showing that 50% of the genes that comprise the "ribosome" KEGG-pathway are increased at the synaptic compartment upon KCL treatment.

Literature

Ainsley JA, Drane L, Jacobs J, Kittelberger KA, Reijmers LG (2014) Functionally diverse dendritic mRNAs rapidly associate with ribosomes following a novel experience. *Nature communications* 5: 4510

Ansari A, Maffioletti, E., Milanesi, E., Marizzoni, M., Frisoni, G. B., Blin, O., Richardson, J. C., Bordet, R., Forloni, G., Gennarelli, M., Bocchio-Chiavetto, L., & PharmaCog Consortium (2019) miR-146a and miR-181a are involved in the progression of mild cognitive impairment to Alzheimer's disease. *Neurobiology of Aging* 82: 102-109

Banzhaf-Strathmann J, Benito E, May S, Arzberger T, Tahirovic S, Kretzschmar H, Fischer A, Edbauer D (2014) MicroRNA-125b induces tau hyperphosphorylation and cognitive deficits in Alzheimer's disease. *EMBO J* 33: 1667-1680

Benito E, Urbanke E, Barth J, Halder R, Capece V, Jain G, Burkhardt S, Navarro M, Schutz AL, Bonn S *et al* (2015) Reinstating transcriptome plasticity and memory function in mouse models for cognitive decline. *J Clin Invest* 125: 3572-3584

Bernard D, Prasanth KV, Tripathi V, Colasse S, Nakamura T, Xuan Z, Zhang MQ, Sedel F, Jourdren L, Coulpier F *et al* (2010) A long nuclear-retained non-coding RNA regulates synaptogenesis by modulating gene expression. . *The EMBO journal* 29: 3082–3093

Biever A, Glock, C., Tushev, G., Ciirdaeva, E., Dalmay, T., Langer, J. D., & Schuman, E. M. (2020). Monosomes actively translate synaptic mRNAs in neuronal processes. Science (New York, N.Y.), 367(6477), eaay4991. (2020) Monosomes actively translate synaptic mRNAs in neuronal processes. *Science* 3677.

Boyken J, Grønborg M, Riedel D, Urlaub H, Jahn R, Chua JJ (2013) Molecular profiling of synaptic vesicle docking sites reveals novel proteins but few differences between glutamatergic and GABAergic synapses. *Neuron* 78: 285-297

Bratkovič T, Božič J, Rogelj B (2020) Functional diversity of small nucleolar RNAs. Nucleic acids research. *Nucleic acids research* 48: 1627-1651

Cajigas IJ, Tushev G, Will TJ, tom Dieck S, Fuerst N, Schuman EM (2012) The local transcriptome in the synaptic neuropil revealed by deep sequencing and high-resolution imaging. . *Neuron* 74: 453–466

Cavaillé J (2017) ox C/D small nucleolar RNA genes and the Prader-Willi syndrome: a complex interplay. . *Wiley interdisciplinary reviews RNA* 8: https://doi.org/10.1002/wrna.1417

599 Chen BJ, Ueberham U, Mills JD, Kirazov L, Kirazov E, Knobloch M, Bochmann J, Jendrek R, Takenaka K,
600 Bliim N *et al* (2017) RNA sequencing reveals pronounced changes in the noncoding transcriptome of aging
601 synaptosomes. *Neurobiology of aging* 56: 67–77
602 Derkow K, Rössling R, Schipke C, Krüger C, Bauer J, Fähling M, Stroux A, Schott E, Ruprecht K, Peters O *et al*
603 (2018) Distinct expression of the neurotoxic microRNA family let-7 in the cerebrospinal fluid of patients with
604 Alzheimer's disease. *PloS one* 13: e0200602
605 Dobin A, Davis CA, Schlesinger F, Drenkow J, Zaleski C, Jha S, Batut P, Chaisson M, Gingeras TR (2013)
606 STAR: ultrafast universal RNA-seq aligner. *Bioinformatics* 13: 673-691
607 Doyle M, Kiebler MA (2011) Mechanisms of dendritic mRNA transport and its role in synaptic tagging. *EMBO*
608 *J* 30: 3540-3552
609 El Fatimy R, Li S, Chen Z, Mushannen T, Gongala S, Wei Z, Balu DT, Rabinovsky R, Cantlon A, Elkhal A *et al*
610 (2018) MicroRNA-132 provides neuroprotection for tauopathies via multiple signaling pathways. *Acta*
611 *Neuropathol* 136: 537-555
612 Farris S, Ward JM, Carstens KE, Samadi M, Wang, Y., Dudek SM (2019) Hippocampal Subregions Express
613 Distinct Dendritic Transcriptomes that Reveal Differences in Mitochondrial Function in CA2. *Cell reports* 29:
614 522–539
615 Fonkeu Y, Kraynyukova N, Hafner AS, Kochen L, Sartori F, Schuman EM, Tchumatchenko T (2019) How
616 mRNA Localization and Protein Synthesis Sites Influence Dendritic Protein Distribution and Dynamics. *Neuron*
617 103: 1109-1122
618 Friedländer MR, Mackowiak SD, Li N, Chen W, Rajewsky N (2012) miRDeep2 accurately identifies known and
619 hundreds of novel microRNA genes in seven animal clades. *Nucleic acids research* 40: 37-52
620 Garner CC, Tucker RP, Matus A (1988) Selective localization of messenger RNA for cytoskeletal protein MAP2
621 in dendrites. *Nature biotechnology*, 336: :674–677
622 Griffiths-Jones S (2006) miRBase: the microRNA sequence database. *Methods in molecular biology*: 129-138
623 Gurtan AM, Sharp PA (2013) The Role of miRNAs in Regulating Gene Expression Networks. *J Mol Biol* pii:
624 Epub ahead of print
625 Hafner AS, Donlin-Asp, P. G., Leitch, B., Herzog, E., & Schuman, E. M. (2019). Local protein synthesis is a
626 ubiquitous feature of neuronal pre- and postsynaptic compartments. Science (New York, N.Y.), 364(6441),
627 eaau3644. (2019) Local protein synthesis is a ubiquitous feature of neuronal pre- and postsynaptic
628 compartments. . *Science* 364: eaau3644
629 Hefter D, Ludewig S, Draguhn A, Korte M (2020) Amyloid, APP, and Electrical Activity of the Brain. . *The*
630 *Neuroscientist* 26: 231-251
631 Holt CE, Martin KC, Schuman EMLtinvafNsmb, 26(7), 557–566. (2019) *Nature structural & molecular biology*
632 26: 557–566.
633 Jain G, Stuendl A, Rao P, Berulava T, Pena Centeno T, Kaurani L, Burkhardt S, Delalle I, Kornhuber J, Hüll M
634 *et al* (2019) A combined miRNA-piRNA signature to detect Alzheimer's disease. . *Translational Psychiatry* 9:
635 250
636 Jose AM (2015) Movement of regulatory RNA between animal cells. . *Genesis* 53: 395-416
637 Jovičić A, Roshan R, Moisoi N, Pradervand S, Moser R, Pillai B, Luthi-Carter R (2013) Comprehensive
638 expression analyses of neural cell-type-specific miRNAs identify new determinants of the specification and
639 maintenance of neuronal phenotypes. *J Neurosci* 33: 5127-5137
640 Karagkouni D, Paraskevopoulou MD, Chatzopoulos S, Vlachos IS, Tastsoglou S, Kanellos I, Papadimitriou D,
641 Kavakiotis I, Maniou S, Skoufos G *et al* (2018) DIANA-TarBase v8: a decade-long collection of experimentally
642 supported miRNA-gene interactions. . *Nucleic acids research* 46: D239–D245
643 Kosik KS (2016) Low Copy Number: How Dendrites Manage with So Few mRNAs. *Neuron* 92: 1168–1180
644 Kye MJ, Liu T, Levy SF, Xu NL, Groves BB, Bonneau R, Lao K, Kosik KS (2007) Somatodendritic
645 microRNAs identified by laser capture and multiplex RT-PCR. *RNA* 13: 1224–1234
646 Langmead B, Salzberg SL (2012) Fast gapped-read alignment with Bowtie 2. *Nat Methods* 9: 357-359
647 Liao Y, Smyth GK, Shi W (2014) featureCounts: an efficient general purpose program for assigning sequence
648 reads to genomic features. *Bioinformatics* 30: 923-930
649 Liu Y, Zhang Y, Liu P, Bai H, Li X, Xiao J, Yuan Q, Geng S, Yin H, Zhang H *et al* (2019) MicroRNA-128
650 knockout inhibits the development of Alzheimer's disease by targeting PPARγ in mouse models. *European*
651 *journal of pharmacology* 843: 132-144
652 Liu ZP, Wu C, Miao H, Wu H (2015) RegNetwork: an integrated database of transcriptional and post-
653 transcriptional regulatory networks in human and mouse. *Database : the journal of biological databases and*
654 *curatio* bav095
655 Love MI, Huber W, Anders S (2014) Moderated estimation of fold change and dispersion for RNA-seq data with
656 DESeq2. *Genome Biol* 15: 550
657 Lugli G, Torvik VI, Larson J, Smalheiser NR (2008) Expression of microRNAs and their precursors in synaptic
658 fractions of adult mouse forebrain. *J Neurochem* 106: 650-661
659 Most D, Ferguson L, Blednov Y, Mayfield RD, Harris RA (2015) The synaptoneurosome transcriptome: a
660 model for profiling the emolecular effects of alcohol. *The pharmacogenomics journal* 15: 177-188

661 Plog BA, Nedergaard M (2018) The glymphatic system in CNS health and disease: past, present and future.
662 *Annu Rev Pathol* 24: 379-394
663 Prada I, Gabrielli M, Turola E, Iorio A, D'Arrigo G, Parolisi R, De Luca M, Pacifici M, Bastoni M, Lombardi M
664 *et al* (2018) Glia-to-neuron transfer of miRNAs via extracellular vesicles: a new mechanism underlying
665 inflammation-induced synaptic alterations. *Acta neuropathologica*, 135: 529-550
666 Rajman M, Schratt G (2017) MicroRNAs in neural development: from master regulators to fine-tuners.
667 *Development* 44: 2310-2322
668 Rao P, Benito E, Fischer A (2013) MicroRNAs as biomarkers for CNS disease. *Front Mol Neurosci* 26:
669 eCollection 2013
670 Risso D, Ngai J, Speed TP, Dudoit S (2014) Normalization of RNA-seq data using factor analysis of control
671 genes or samples. *Nature biotechnology* 32: 896
672 Rupaimoole R, Slack F, J. (2017) MicroRNA therapeutics: towards a new era for the management of cancer and
673 other diseases. . *Nat Rev Drug Discov* 16: 203-222
674 Sambandan S, Akbalik G, Kochen L, Rinne J, Kahlstatt J, Glock C, Tushev G, Alvarez-Castelao B, Heckel A,
675 Schuman EM (2017) Activity-dependent spatially localized miRNA maturation in neuronal dendrites. *Science*
676 355: 634-637
677 Shannon P, Markiel A, Ozier O, Baliga NS, Wang JT, Ramage D, Amin N, Schwikowski B, Ideker T (2003)
678 Cytoscape: a software environment for integrated models of biomolecular interaction networks. *Genome*
679 *research* 13: 2498.2504
680 Smalheiser NR (2014) The RNA-centred view of the synapse: non-coding RNAs and synaptic plasticity. *Philos*
681 *Trans R Soc Lond B Biol Sci* 369: pii: 20130504
682 Smalheiser NR, Lugli G, Zhang H, Rizavi H, Cook EH, Dwivedi Y (2014) Expression of microRNAs and other
683 small RNAs in prefrontal cortex in schizophrenia, bipolar disorder and depressed subjects. *PLoS One* 9: e86469
684 Smythies J, Edelstein L (2013) Transsynaptic modality codes in the brain: possible involvement of synchronized
685 spike timing, microRNAs, exosomes and epigenetic processes. *Frontiers in integrative neuroscience* 6:
686 https://doi.org/10.3389/fnint.2012.00126
687 Sotelo JR, Canclini L, Kun A, Sotelo-Silveira JR, Calliari A, Cal K, Bresque M, Dipaolo A, Farias J, Mercer JA
688 (2014) Glia to axon RNA transfer. . *Developmental neurobiology* 73: 292-302
689 Stepniak B, Kästner A, Poggi G, Mitjans M, Begemann M, Hartmann A, Van der Auwera S, Sananbenesi F,
690 Krueger-Burg D, Matuszko G *et al* (2015) Accumulated common variants in the broader fragile X gene family
691 modulate autistic phenotypes. *EMBO Mol Med* 7: 1565-1579
692 Szklarczyk D, Gable AL, Lyon D, Junge A, Wyder S, Huerta-Cepas J, Simonovic M, Doncheva NT, Morris JH,
693 Bork P *et al* (2019) STRING v11: protein-protein association networks with increased coverage, supporting
694 functional discovery in genome-wide experimental datasets. *Nucleic Acids Res* 47: D607-D613
695 Taylor AM, Dieterich DC, Ito HT, Kim SA, Schuman EM (2010) Microfluidic local perfusion chambers for the
696 visualization and manipulation of synapses. *Neuron, 66(1), 57–68* 66: 57–68
697 Teng X, Chen X, Xue H, Tang Y, Zhang P, Kang Q, Hao Y, Chen R, Zhao Y, He S (2020) NPInter v4.0: an
698 integrated database of ncRNA interactions. *Nucleic acids research* 48: 160-165
699 Tong Z, Cui Q, Wang J, Zhou Y (2019) TransmiR v2.0: an updated transcription factor-microRNA regulation
700 database. *Nucleic acids research* 47: D253–D258
701 Valadi H EK, Bossios A, Sjöstrand M, Lee JJ, Lötvall JO. (2007) Exosome-mediated transfer of mRNAs and
702 microRNAs is a novel mechanism of genetic exchange between cells. *Nat Cell Biol* 9: 654-659
703 Weiss K, Antoniou A, Schratt G (2015) Non-coding mechanisms of local mRNA translation in neuronal
704 dendrites. *European journal of cell biology* 94: 363-367
705 Xu J, Chen Q, Zen K, Zhang C, Zhang Q (2013) Synaptosomes secrete and uptake functionally active
706 microRNAs via exocytosis and endocytosis pathways. *J Neurochem* 124: 15-25
707 Yoshihama M, Nakao A, Kenmochi N (2013) snOPY: a small nucleolar RNA orthological gene database. *BMC*
708 *research notes* 6
709

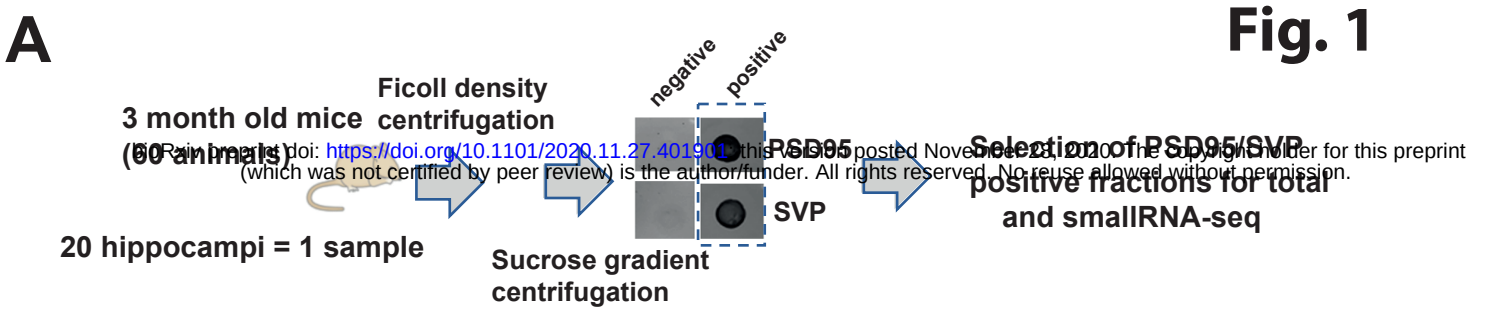

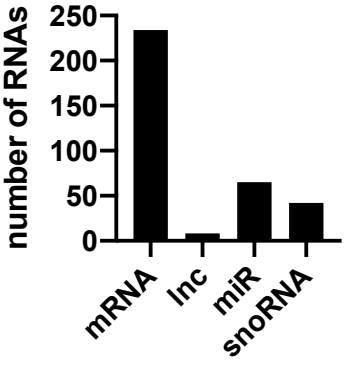

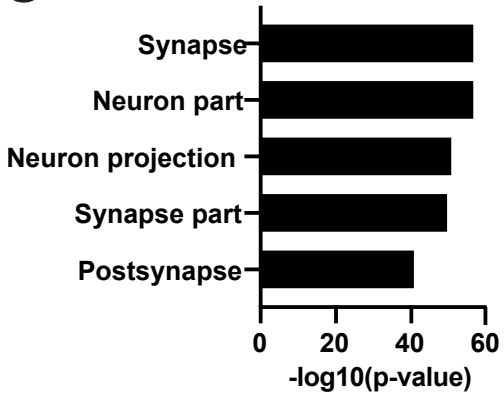

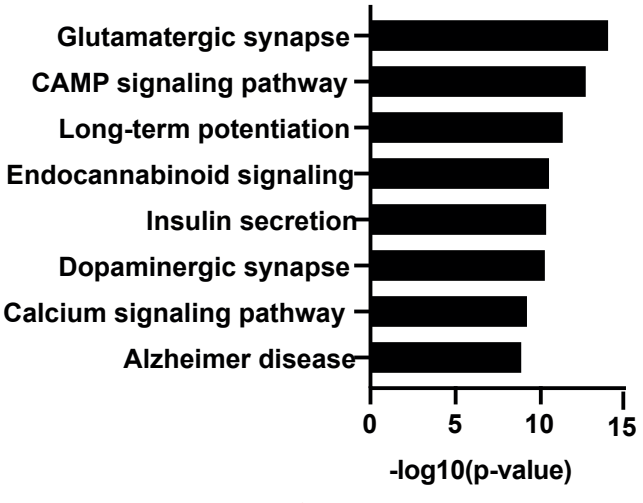

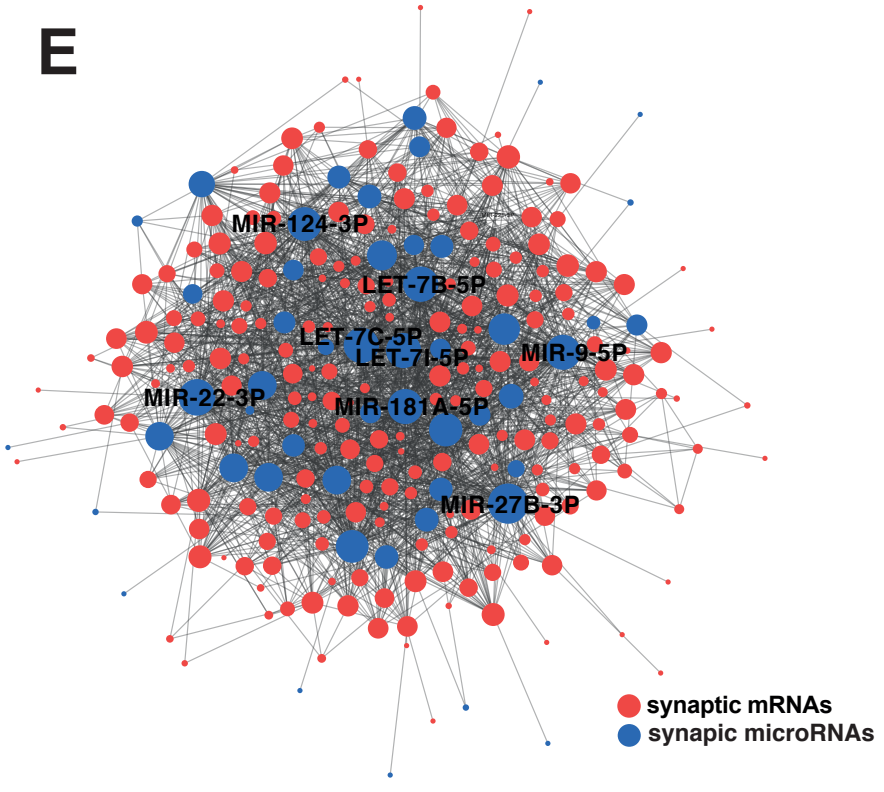

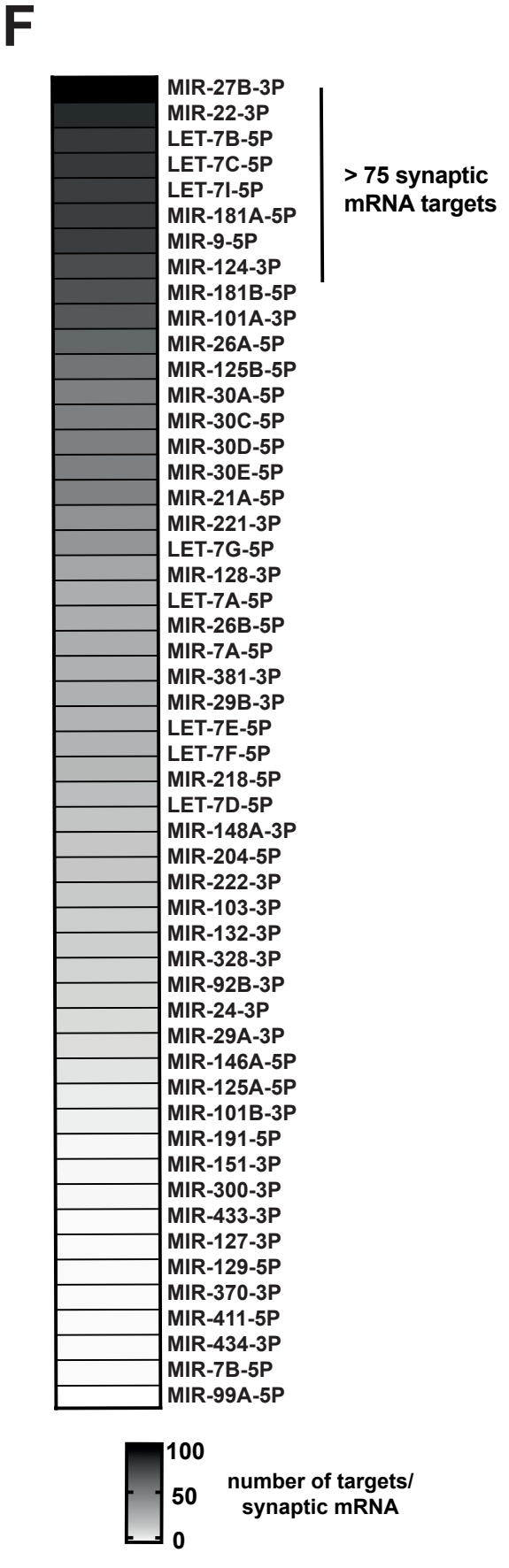

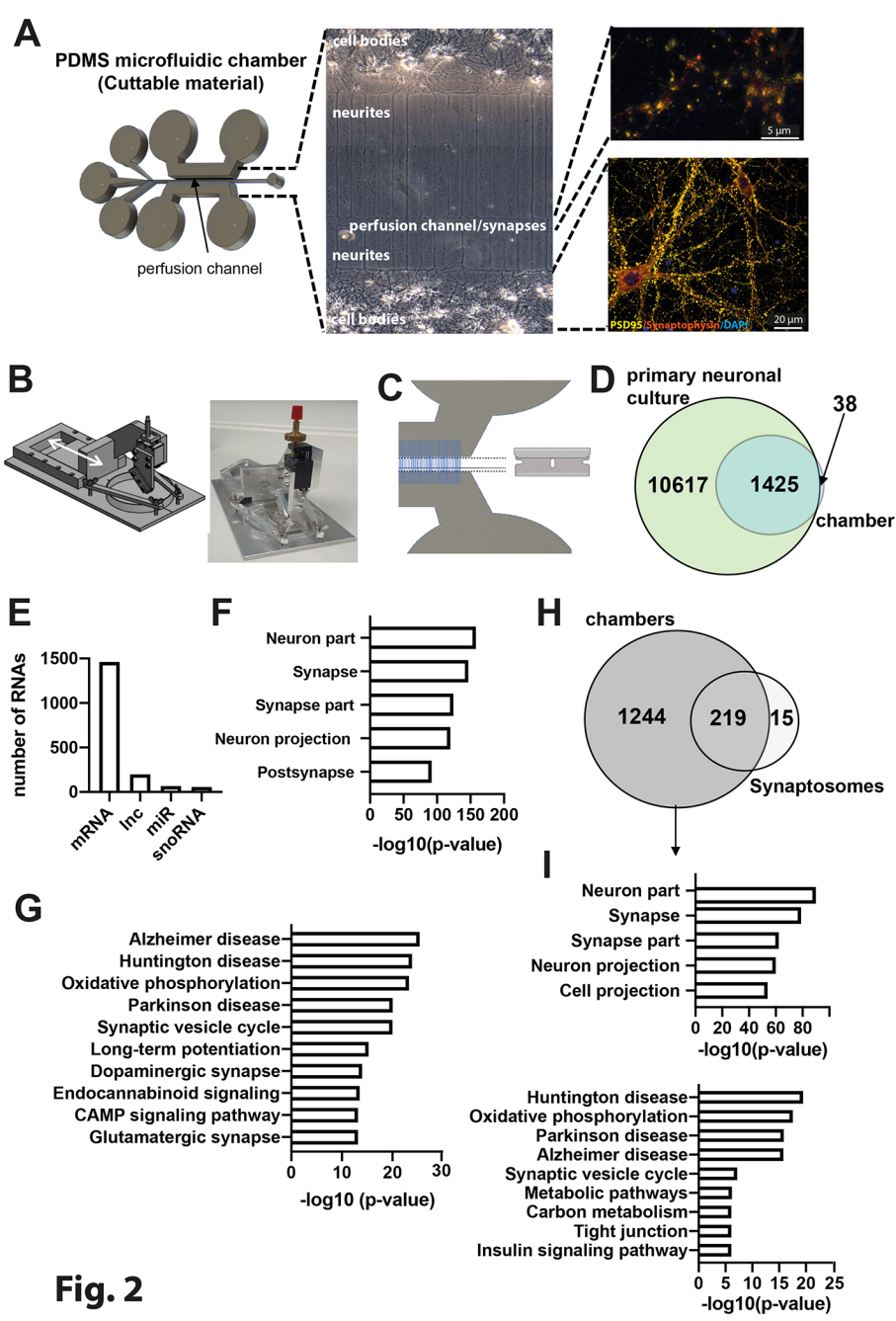
A
PDMS microfluidic chamber
(Cuttable material)
perfusion channel
cell bodies
neurites
perfusion channel/synapses
neurites
cell bodies
5 µm
PSD95/Synaptophysin/DAPI
20 µm
B
C
D
primary neuronal culture
10617
1425
38
chamber
E
number of RNAs
1500
1000
500
0
mRNA
lnc
miR
snoRNA
F
Neuron part
Synapse
Synapse part
Neuron projection
Postsynapse
0 50 100 150 200
-log10(p-value)
H
chambers
1244
219
15
Synaptosomes
I
Neuron part
Synapse
Synapse part
Neuron projection
Cell projection
0 20 40 60 80
-log10(p-value)
G
Alzheimer disease
Huntington disease
Oxidative phosphorylation
Parkinson disease
Synaptic vesicle cycle
Long-term potentiation
Dopaminergic synapse
Endocannabinoid signaling
CAMP signaling pathway
Glutamatergic synapse
0 10 20 30
-log10 (p-value)
Huntington disease
Oxidative phosphorylation
Parkinson disease
Alzheimer disease
Synaptic vesicle cycle
Metabolic pathways
Carbon metabolism
Tight junction
Insulin signaling pathway
0 5 10 15 20 25
-log10(p-value)

Fig. 2

Fig. 3

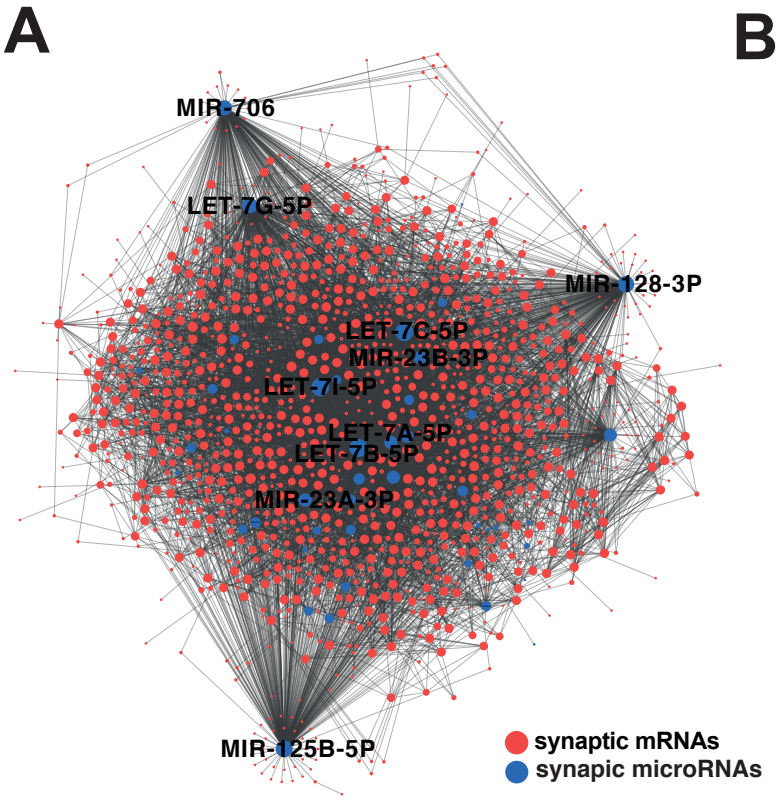

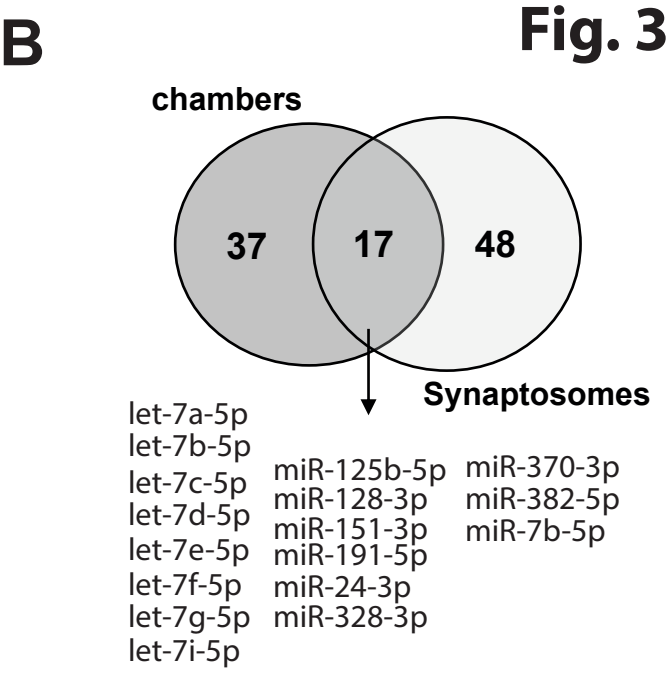

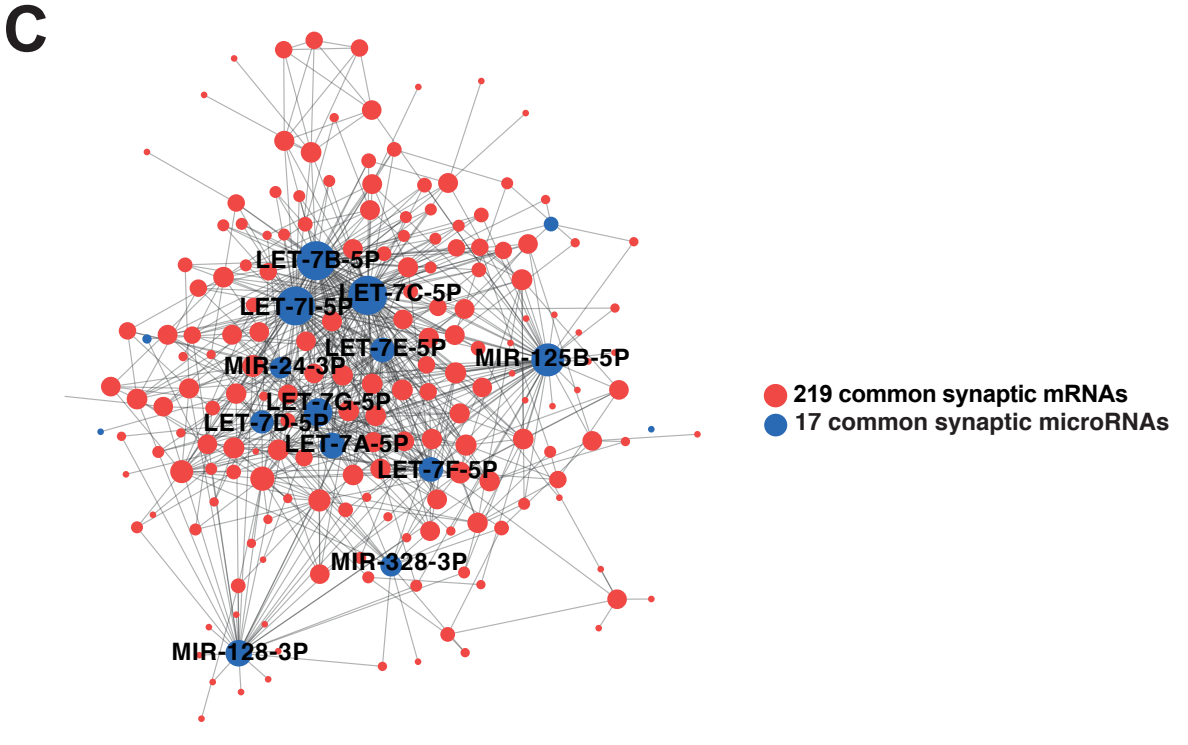

A

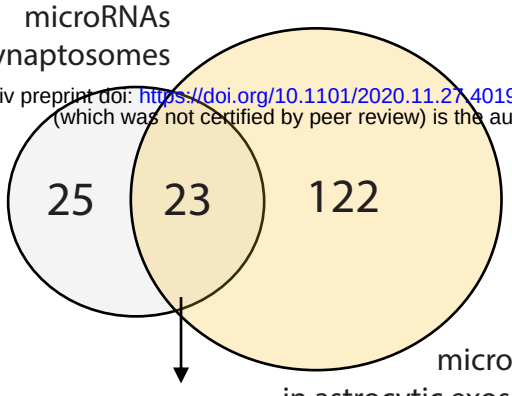

miR-99b-5p	miR-30c-5p	miR-222-3p
miR-9-5p	miR-30a-5p	miR-221-3p
miR-7a-5p	miR-132-3p	miR-218-5p
miR-434-3p	miR-29a-3p	miR-146a-5p
miR-411-5p	miR-29b-3p	miR-127-3p
miR-381-3p	miR-27b-3p	miR-101b-3p
miR-30e-5p	miR-26a-5p	miR-100-5p
miR-30d-5p	miR-26b-5p	

B

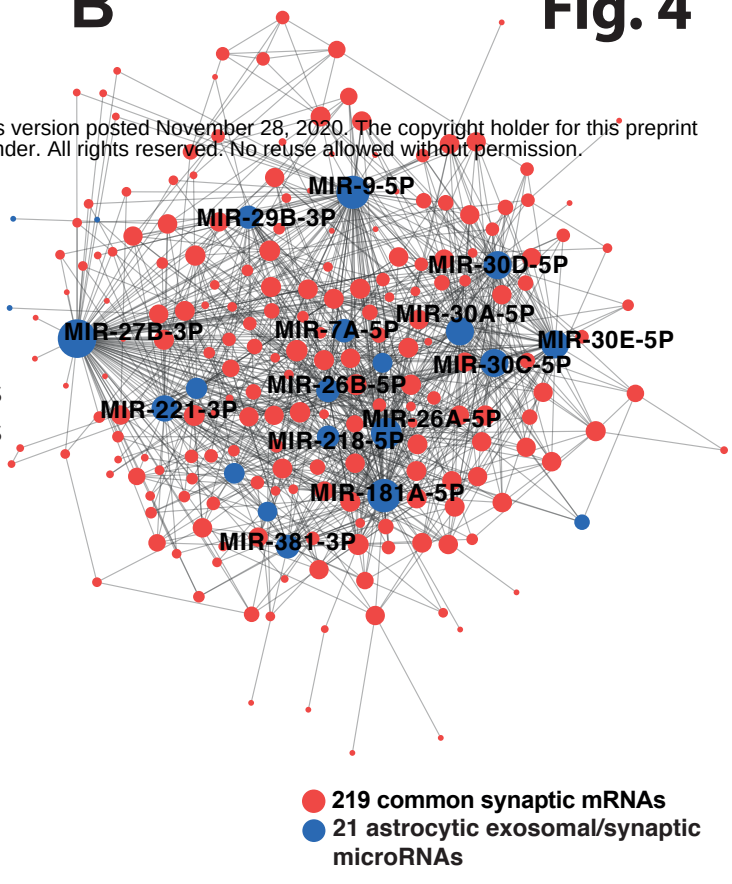

C

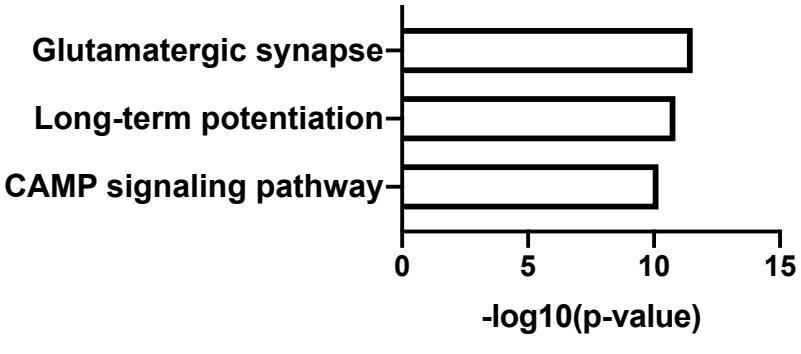

D

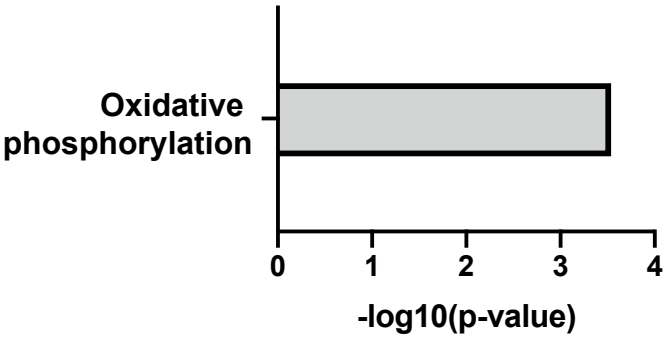

Fig. 5

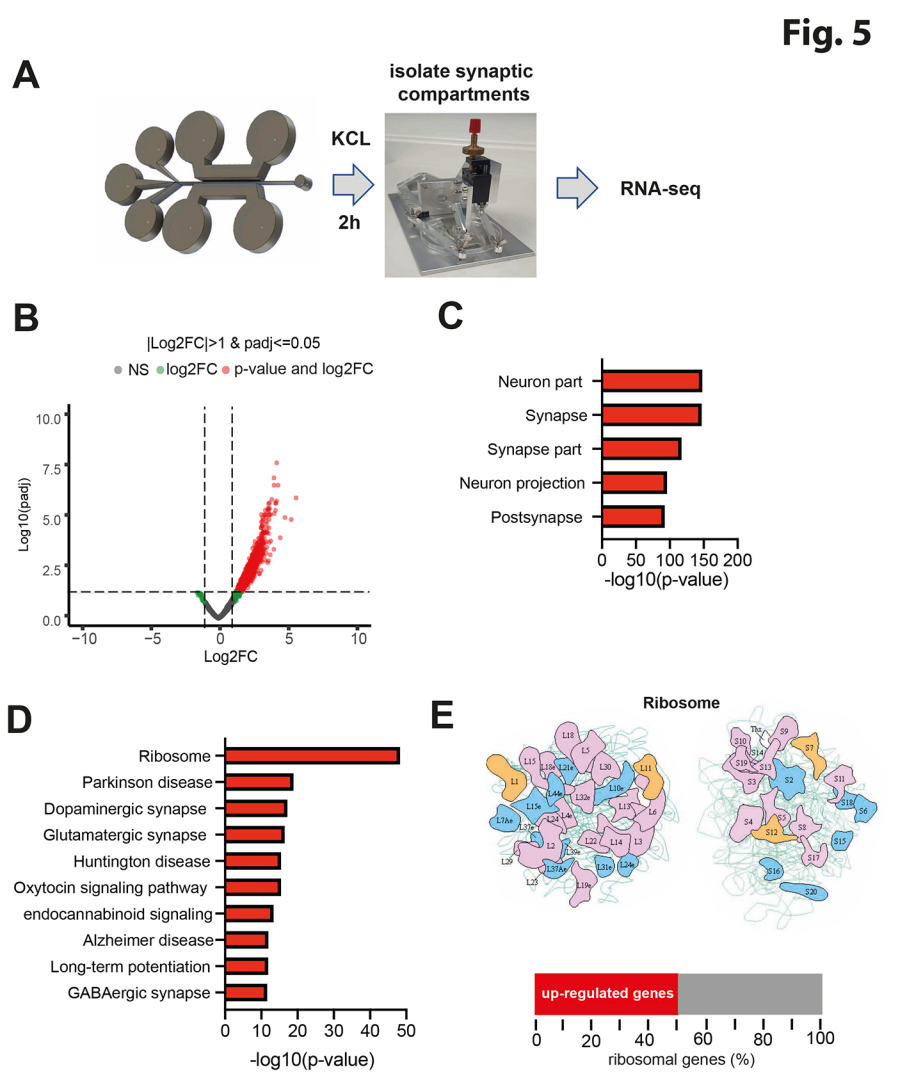
A
isolate synaptic compartments
KCL
2h
RNA-seq
B
|Log2FC|>1 & padj<=0.05
NS
log2FC
p-value and log2FC
Log10(padj)
Log2FC
C
Neuron part
Synapse
Synapse part
Neuron projection
Postsynapse
-log10(p-value)
D
Ribosome
Parkinson disease
Dopaminergic synapse
Glutamatergic synapse
Huntington disease
Oxytocin signaling pathway
endocannabinoid signaling
Alzheimer disease
Long-term potentiation
GABAergic synapse
-log10(p-value)
E
Ribosome
up-regulated genes
ribosomal genes (%)